Journal of Photochemistry and Photobiology B: Biology 138 (2014) 273–281

Contents lists available at ScienceDirect

Journal of Photochemistry and Photobiology B: Biology

journal homepage: www.elsevier.com/locate/jphotobiol

Influence of light history on the photosynthetic and motility responses of *Gymnodinium chlorophorum* exposed to UVR and different temperatures

Donat-P. Häder [a,*], Peter R. Richter [b,1], Virginia E. Villafañe [c,2], E. Walter Helbling [c,2]

[a] Neue Str. 9, 91096 Möhrendorf, Germany
[b] Friedrich-Alexander Universität, Department Biologie, Lehrstuhl für Zellbiologie, AG für Gravitationsbiologie, Staudtstr. 5, 90158 Erlangen, Germany
[c] ESTACIÓN de Fotobiología Playa Unión, Casilla de Correo 15, U9103ZAA Rawson, Chubut, Argentina

ARTICLE INFO

Article history:
Received 25 March 2014
Received in revised form 20 May 2014
Accepted 26 May 2014
Available online 17 June 2014

Keywords:
Gymnodinium chlorophorum
Global change
UVR
Effective photochemical quantum yield
Electron transport vs. irradiance
Temperature

ABSTRACT

In the wake of global climate change, phytoplankton productivity and species composition is expected to change due to altered external conditions such as temperature, nutrient accessibility, pH and exposure to solar visible (PAR) and ultraviolet radiation (UVR). The previous light history is also of importance for the performance of phytoplankton cells. In order to assess the combined impacts of UVR and temperature on the dinoflagellate *Gymnodinium chlorophorum* we analyzed the effective photochemical quantum yield (*Y*), relative electron transport rate vs. irradiance curves (rETR vs. I), percentage of motile cells and swimming velocity. Cells were grown at three different temperatures (15, 20 and 25 °C) and two PAR intensities: low light (LL, 100 μmol photons m^{-2} s^{-1}) and high light (HL, 250 μmol photons m^{-2} s^{-1}). Pre-acclimated cells were then exposed to either PAR only (P), PAR + UV-A (PA) or PAR + UV-A + UV-B (PAB) radiation at two different irradiances, followed by a recovery period in darkness. The *Y* decreased during exposure, being least inhibited in P and most in PAB treatments. Inhibition was higher and recovery slower in LL-grown cells than in HL-grown cells at 15° and 20 °C, but the opposite occurred at 25 °C, when exposed to high irradiances. Maximal values of rETR were determined at t_0 as compared to the different (before and after exposure) radiation treatments. The effects of temperature and UVR on rETR were antagonistic in LL-grown cells (i.e., less UVR inhibition at higher temperature), while it was synergistic in HL cells. Swimming velocity and percentage of motile cells were not affected at all tested temperatures and exposure regimes, independent of the light history. Our results indicate that, depending on the previous light history, increased temperature and UVR as predicted under climate change conditions, can have different interactions thus conditioning the photosynthetic response of *G. chlorophorum*.

1. Introduction

Phytoplankton are the major biomass producers in aquatic ecosystems, being responsible for about half of the biological uptake of atmospheric CO_2 [1]. Even though their standing crop is only about 1% of that of all plants, their primary productivity equals that of all terrestrial ecosystems taken together [2,3].

In addition to picoplanktonic cyanobacteria and diatoms, dinoflagellates play a key ecological role at the base of the food web [1]. Furthermore they constitute important components of the microbial loop [4] and, as zooxanthellae, they play a central role in building-up coral reefs [5]. Dinoflagellates often cause red tides, generally blooms of toxic organisms in coastal waters [6], which are responsible for poisoning of humans and animals after ingestion [7–9]. The occurrence of these harmful algal blooms has increased since the cysts of these dinoflagellates are spread globally being carried by marine transport in ballast water [10] and the severity of the blooms is enhanced by increasing temperatures as expected in a global climate change scenario [8].

While some dinoflagellates are heterotrophic [11,12], most use photosynthesis for their energy generation. For this they have to dwell in the photic zone where they are simultaneously exposed to solar ultraviolet radiation (UVR, 280–400 nm). In the past years

* Corresponding author. Tel.: +49 9131 48730.
E-mail addresses: donat@dphaeder.de (Donat-P. Häder), Peter.richter@fau.de (P.R. Richter), efpu@efpu.org.ar (V.E. Villafañe), whelbling@efpu.org.ar (E.W. Helbling).
URLs: http://www.dphaeder.de (Donat-P. Häder), http://www.zellbio.nat.uni-erlangen.de (P.R. Richter), http://www.efpu.org.ar (V.E. Villafañe), http://www.efpu.org.ar (E.W. Helbling).
[1] Tel.: +49 9131 8528222; fax: +49 9131 8528215.
[2] Tel.: +54 (280) 4498019.

http://dx.doi.org/10.1016/j.jphotobiol.2014.05.020
1011-1344/

the bloom-forming dinoflagellate *Gymnodinium* [13–15] has received considerable attention, with many studies evaluating the effects of different variables and stressors on its physiology and ecology [16–18]. Also, a number of studies have investigated the effects of UVR on different species of *Gymnodinium* and have highlighted the variability in its responses, depending on the target being involved [19–21]. For example, in experiments carried out with *G. breve* Evens et al. [22] determined that this species was rather resistant to UVR exposure in terms of the epoxidation state of xanthophyll cycle pigments as well as maximum quantum yield. On the other hand, and when evaluating the effects of UVR on the motility of *Gymnodinium chlorophorum*, Richter et al. [23] found a slight decrease in swimming speed and percentage of motile cells after UVR exposure.

The observed responses can be also affected by the synergistic or antagonistic influence of different variables [24] i.e., responses to single stressors may be different when analyzed using a multivariable approach. This is particularly interesting in the context of global change, where variables associated with this process e.g., temperature, mixing, nutrients and UVR, among others, are expected to considerably change, thus affecting significantly responses of phytoplankton organisms [1] including dinoflagellates [25]. Working with *G. sanguineum*, Litchman et al. [26] found that nitrogen-limited cultures were more sensitive to UVR than those grown in N-replete media. This was attributed to a reduced synthesis of mycosporine-like amino acids (MAAs), which act as sunscreens in this species [26], in the N-limited cultures, thereby reducing the photoprotection potential of these compounds as well as causing changes in both defense and repair mechanisms. Doyle et al. [27] observed a growth reduction in *Gymnodinium* sp. when exposed to UVR at lower, but not at higher temperatures without nutrient addition. Helbling et al. [20] found that artificially increased mixing speed within the upper mixed layer significantly increased UVR-induced inhibition of carbon fixation in *G. chlorophorum*.

The aim of our study was to determine the combined effects of global change variables (i.e., increased radiation and temperature) on a dinoflagellate grown with different light histories. We used a key model organism such as *G. chlorophorum*, which is known to cause blooms in coastal waters [15,28]. Specifically, the present study was designed to assess the impact of increased UVR and temperatures levels on two important physiological targets, photosynthesis and motility. Often exposure experiments are carried out with cultures grown under defined light and temperature conditions. Since the light history plays an important role in the response to external stress factors, due to the adaptation capabilities of the organisms, we grew the cells at either low (LL) or high light (HL) irradiances, and then exposed them to increased irradiances, simulating a decrease in the upper mixed layer (UML) depth (which will cause a higher irradiance exposure by phytoplankton cells) as they would occur under an increasing temperature scenario [29].

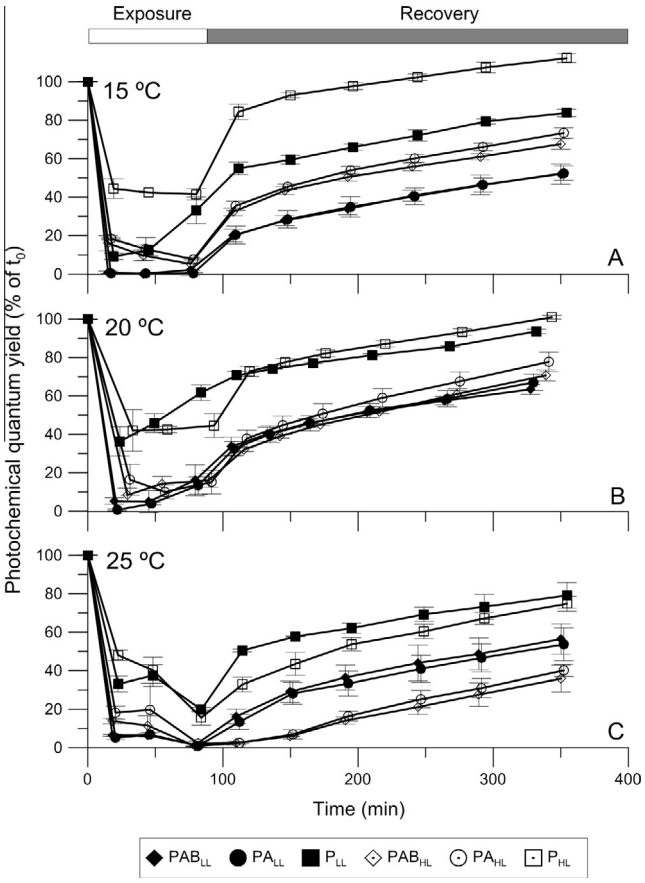

Fig. 1. Effective photochemical quantum yield (percentage of values at time zero), at three different temperatures, of cultures exposed at 95 cm from the solar simulator under three radiation treatments, receiving 184 (846 µmol photons m^{-2} s^{-1}), 35 and 0.64 W m^{-2} for PAR, UV-A and UV-B, respectively. Closed and open symbols represent LL- (100 µmol photons m^{-2} s^{-1}) and HL- (250 µmol photons m^{-2} s^{-1}) acclimated samples, respectively. Symbols indicate mean values of the different radiation treatments (P squares, PA circles, PAB diamonds) with standard deviation.

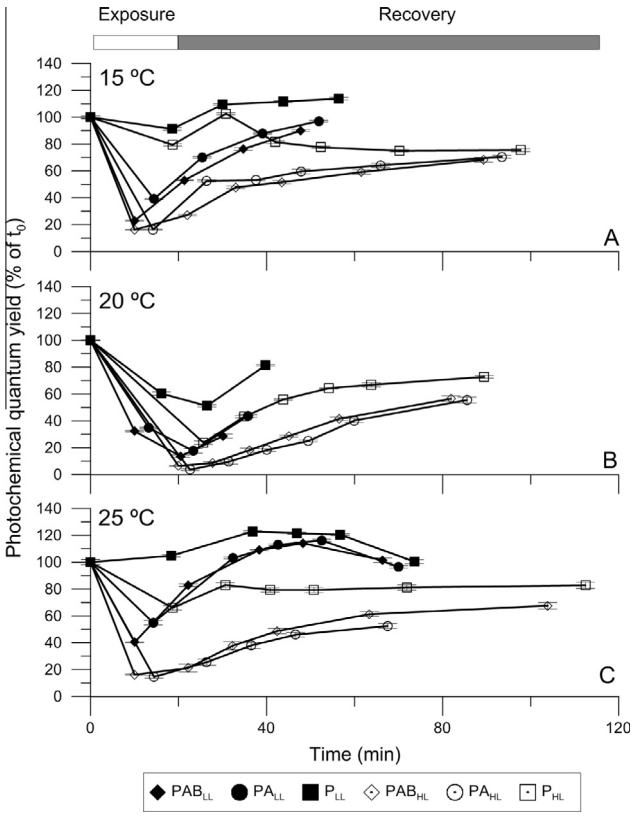

Fig. 2. Effective photochemical quantum yield (percentage of values at time zero), at three different temperatures, of LL pre-acclimated cultures (black symbols) exposed to 146 (671 µmol photons m^{-2} s^{-1}), 27 and 0.5 W m^{-2} for PAR, UV-A and UV-B, respectively, and HL pre-acclimated cultures (open symbols) exposed to 268 (1232 µmol photons m^{-2} s^{-1}), 49 and 0.89 W m^{-2} for PAR, UV-A and UV-B, respectively. Symbols indicate mean values of the different radiation treatments (P squares, PA circles, PAB diamonds) with standard deviation.

2. Materials and methods

2.1. Culture conditions

The dinoflagellate *G. chlorophorum*, Elbrächter & Schnepf was obtained from the Culture Collection at the Friedrich-Alexander Universität (FAU, Erlangen, Germany) and grown in f/2 medium [30]. Cultures were pre-acclimated for at least a week in a culture chamber at three different temperatures: 15, 20, 25 °C and under two irradiances: 100 (LL) and 250 (HL) μmol photons m^{-2} s^{-1} provided by six daylight fluorescent tubes. The idea behind the pre-acclimation to two irradiances i.e., low light (LL) and high light (HL) was to have cultures with two different light history conditions, one below and one above the light saturation parameter (I_k), that was determined in preliminary measurements done with the cultures growth conditions at FAU. An additional temperature was also tested i.e., 30 °C, but since the cultures did not grow, experiments were not conducted under this condition.

2.2. Experimental conditions/sampling protocols

The cultures were placed in 50 ml quartz tubes and incubated at the corresponding growth temperature under a solar simulator (SOL 1200, Hönle System, Martinsried, Germany). Three radiation treatments were established: P [photosynthetic active radiation (PAR), 400–700 nm] using tubes covered with Ultraphan UV Opak 395 filter; PA [PAR + UV-A (ultraviolet A), 315–700 nm) using tubes covered with Montagefolie 320 filter, and PAB [PAR + UV-A + UV-B (ultraviolet B), 280–700 nm], using tubes covered with Ultraphan 290 or acetate film to screen out UV-C emitted by the solar simulator]. Two types of experiments were done, in which we increased the amount of radiation received by the cells, thus simulating a decrease in the UMLs depth. The conditions simulated in our experiments described below correspond to changes in the UML as those previously found at mid-latitudes during summer due to transient thermoclines [31], and as predicted due to an increase in temperature [29].

Experiment 1 (E1): Cultures, pre-acclimated either to LL or HL, were exposed at a distance of 95 cm from the solar simulator, under three radiation treatments (PAB, PA, and P), receiving 184 (846 μmol photons m^{-2} s^{-1}), 35 and 0.64 W m^{-2} for PAR, UV-A and UV-B, respectively, for 75 min, and then transferred to dim light for recovery. Samples for measurements of different Chl *a* fluorescence parameters (see below) during the exposure period were taken at t_0, 15, 40 and 75 min and then every 40–50 min during the recovery phase in dim light (see below). This experiment was designed to evaluate the role of previous light history (i.e., LL and HL) in the responses of cells when exposed to common

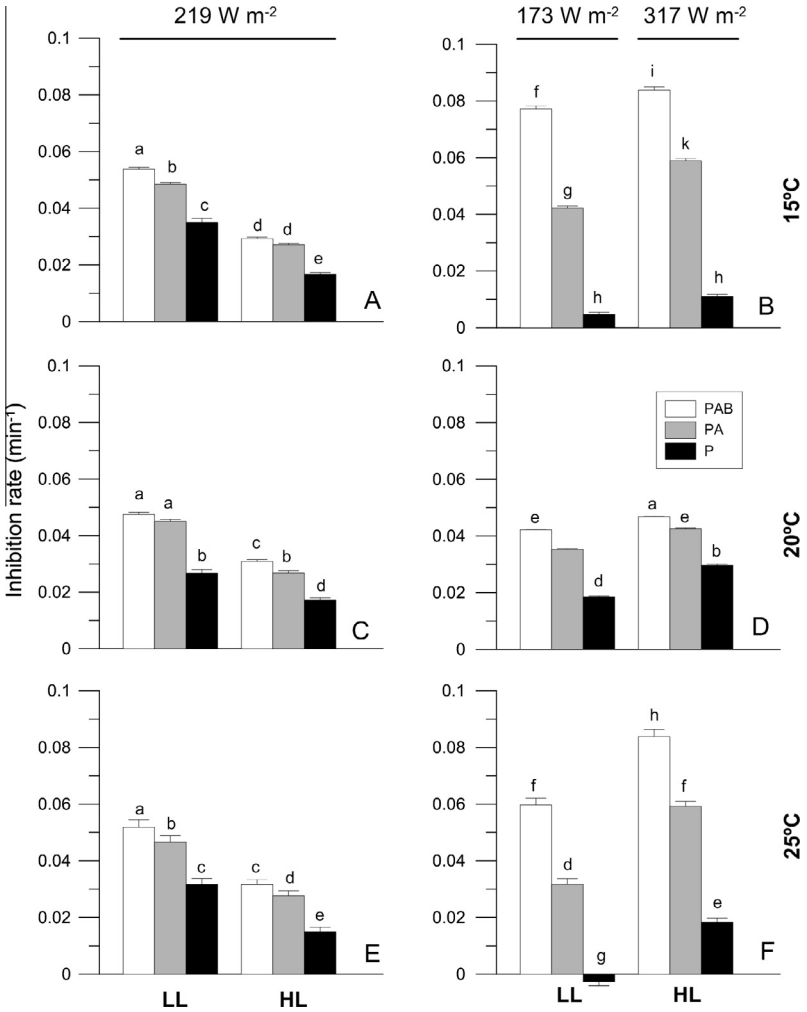

Fig. 3. Inhibition rates (min^{-1}) at three different temperatures for HL- or LL-acclimated samples exposed at 95 cm from the solar simulator thus receiving a total radiation of 219 Wm^{-2} (A, C, and E) or LL- and HL- acclimated samples exposed at 105 cm or 80 cm from the solar simulator, respectively, thus receiving total radiation of 173 or 317 W m^{-2}, respectively (B, D, and F), under three radiation treatments (PAB, PA, and P). The bars show mean values with standard deviation. The letters indicate the result of the post hoc analyses within each temperature.

increased irradiances. These irradiances simulated the mean radiation levels received by cells in an UML of ~2 m depth, at noon and with an attenuation coefficient for PAR (k_{PAR}) of 1 m^{-1} [32].

Experiment 2 (E2): Cultures, pre-acclimated to LL were exposed to 146 (671 μmol photons m^{-2} s^{-1}), 27 and 0.5 W m^{-2} for PAR, UV-A and UV-B, respectively, at 105 cm distance from the solar simulator, while HL pre-acclimated cultures were exposed to 268 (1232 μmol photons m^{-2} s^{-1}), 49 and 0.89 W m^{-2} for PAR, UV-A and UV-B, respectively, at 80 cm distance from the solar simulator. After 20 min of exposure the samples were transferred to dim light for recovery. Samples for measurements of Chl *a* fluorescence parameters (see below) were taken at t_0, 10 and 20 min during the exposure, and every ca. 15 min during recovery. In these experiments we simulated a decrease of the UML depth by exposing samples pre-acclimated to LL to a mean irradiance in a UML of ~3 m depth, while in the case of HL samples we simulated a UML of ~1 m depth.

2.3. Analysis and measurements

2.3.1. Photosynthesis

Chl *a* fluorescence parameters were measured *in vivo* with a pulse amplitude-modulated (PAM) fluorometer (Walz, Water PAM, Effeltrich, Germany). Briefly, 3-ml aliquots were placed in a cuvette and measured 4–6 times immediately after sampling. The effective photochemical quantum yield (Y) was calculated using the equations of Genty et al. [33] and Weis and Berry [34] as:

$$Y = \Delta F/F'_m = (F'_m - F_t)/F'_m \quad (1)$$

where F'_m is the maximum fluorescence induced by a saturating light pulse (ca. 5300 μmol photons m^{-2} s^{-1} for 0.8 s) and F_t the current steady state fluorescence induced by an actinic light in light-adapted cells. Other photosynthetic parameters, such as non photochemical quenching (NPQ), were calculated using the software provided by the manufacturer.

Relative electron transport rate (rETR) vs. I curves were obtained at the beginning and at the end of the exposure period by exposing the samples to increasing irradiances from 0 to 1818 μmol photons m^{-2} s^{-1} with the PAM fluorometer. The data were analyzed and fitted, and parameters such as α (the light-limited slope of the ETR vs. I curve), ETR_{max} (the maximum electron transport rate) and I_k (the light saturation parameter, i.e. the intercept between the initial slope of the ETR vs. I curve and ETR_{max}) were calculated using the equations of Eilers and Peeters [35].

2.3.2. Motility and swimming velocity

Samples were collected at the same time when chl *a* fluorescence was determined (see above) and transferred into a custom-made observation chamber (0.1 mm depth × 20 mm diameter) made from stainless steel with glass windows (Daimler-Benz

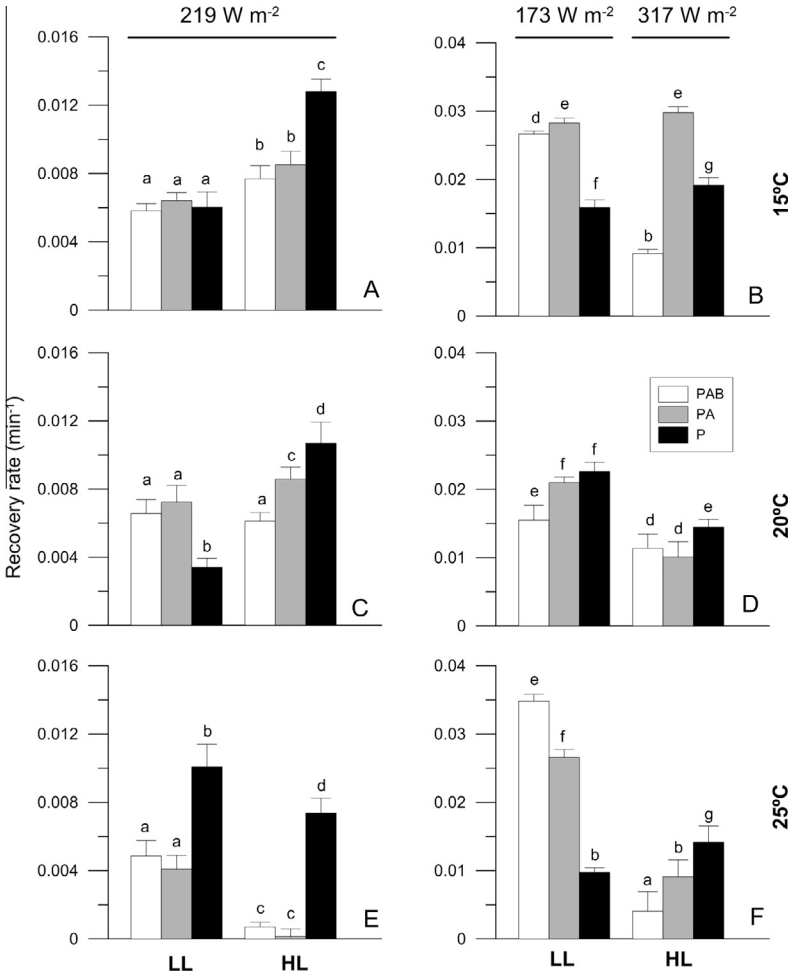

Fig. 4. Recovery rates (min^{-1}) at three different temperatures for HL- or LL-acclimated samples exposed at 95 cm from the solar simulator thus receiving a total radiation of 219 Wm^{-2} (A, C, and E) or LL- and HL- acclimated samples exposed at 105 cm or 80 cm from the solar simulator, respectively, thus receiving total radiation of 173 or 317 W m^{-2}, respectively (B, D, and F), under three radiation treatments (PAB, PA, and P). The bars show mean values with the standard deviation. The letters indicate the result of the post hoc analyses within each temperature.

Aerospace, Bremen, Germany). The number of motile cells and their swimming velocity was quantified under a microscope using a cell tracking system (WinTrack 2000, Real Time Computer, Möhrendorf, Germany) [36]. Movement analysis was done with the 'track module' of the software, and at least 10 fields of view were analyzed for each sample. Image analysis was done in darkness in order not to induce any phototactic or photophobic response of the cells. Before the measurements the field of view was calibrated with an object micrometer so that the software could calculate real physical values (cell size, cells per volume, velocity etc.).

2.3.3. Statistics and calculations

Duplicate samples from the different radiation treatments and temperatures were used and the experiments were performed twice for each pre-acclimation condition. Thus, four values of the diverse chl *a* fluorescence parameters were obtained for each treatment. The data are presented as means and standard deviation.

The reduction (inhibition) in the effective photochemical quantum yield (Y) was calculated by comparing the initial value (Y_{t0}) and the lowest one during the exposure for each treatment (Y_{t1}), and normalized to the time lapse between them:

$$\text{decrease rate of } Y = (Y_{t0} - Y_{t1})/(t_1 - t_0) \quad (2)$$

The increase (recovery) rate of Y at the end of the dark phase was calculated as:

$$\text{increase rate of } Y = (Y_{tr} - Y_{t1})/(t_r - t_1) \quad (3)$$

where Y represents the effective photochemical quantum yield under a particular radiation treatment (P, PA or PAB), and t_r represents the time at the end of the "recovery" phase.

A one-way repeated measurements ANOVA was used to determine if there were significant differences in Y among radiation treatments within the same temperature. A three way-ANOVA was used to determine significant interactions between temperature, radiation and pre-acclimation conditions on inhibition and recovery of yield, and on swimming velocity. When significant differences were determined, a post hoc Fisher LSD test was performed.

3. Results

Values of Y (as % with respect to t_0) during the E1 experiments are shown in Fig. 1. The initial Y values for LL- and HL-acclimated samples were 0.32–0.35, 0.38–0.38 and 0.27–0.35 for 15, 20 and 25 °C, respectively. The general pattern showed a sharp decay in Y during the first minutes of exposure for all treatments, with samples under the P treatment being significantly ($p < 0.05$) less inhibited (within the same temperature treatment) than those in the PA or PAB treatments. After the initial Y decay, and towards the end of the exposure, no further decrease or even an increase in the percentage of Y was observed for the samples at 15 and 20 °C (Fig. 1A and B), while a continuous decrease was observed at 25 °C (Fig. 1C). During the recovery phase in dim light Y increased for all treatments; however, significant differences were observed among different temperatures. For example, while HL-acclimated samples reached higher Y values (within the same radiation treatment) than LL samples at 15 °C (Fig. 1A), the opposite was observed at 25 °C (Fig. 1C), with LL-acclimated samples reaching higher Y values than the HL-acclimated ones. No significant differences were observed between LL and HL samples at 20 °C (Fig. 1B).

In the E2 experiments (Fig. 2) the cells were exposed to two irradiances of PAR, UV-A and UV-B and for shorter periods of time than in E1. The initial Y values were 0.44, 0.51 and 0.43 for 15, 20 and 25 °C, respectively. As during E1, a strong decay in Y was observed during the first minutes of exposure, which was especially evident at 15 °C (Fig. 2A) in the PA and PAB treatments. In the samples under the P treatment, however, the reduction in the percentage of Y was comparatively small. The observed decrease of Y continued towards the end of the exposure at 20 °C (Fig. 2B), while an increase in the percentage of Y after the initial decay was observed in samples incubated at 15 °C and 25 °C (Fig. 2A and C). For this experiment, the general trend was (within all temperature treatments) to higher Y values (and in general better photosynthetic performance) in samples pre-acclimated to LL.

The inhibition and recovery rates for the two experiments are summarized in Figs. 3 and 4. There were significant interactions between UVR, temperature and irradiance conditions on their impact on inhibition rates ($p < 0.05$). The inhibition rates (Fig. 3) show a clear trend with maximum inhibition rates in the PAB treatment, followed by the PA, and lowest inhibition in the P treatment (Fig. 3). At all experimental irradiances (but more evident in samples exposed to the lowest and highest irradiances) inhibition rates were lower in samples exposed at 20 °C than for those at 15° or 25°. Recovery rates (Fig. 4) were rather similar for all experimental conditions in E1, i.e., light history, radiation and temperature (Figs. 4A, C and E) showing increased values of Y of about 0.008 min^{-1}. However, and with a few exceptions, higher recovery

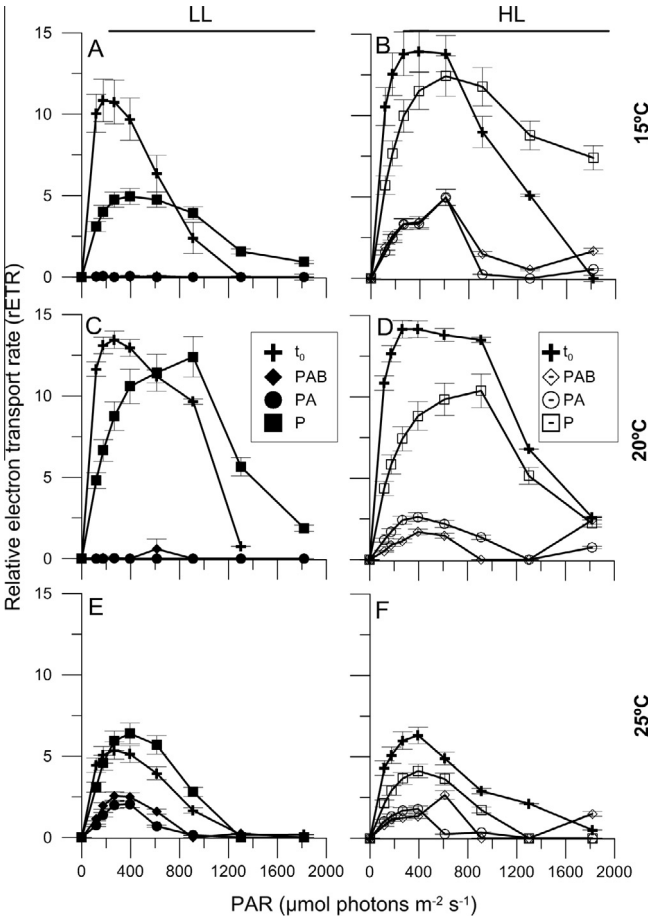

Fig. 5. Relative ETR vs. irradiance curves, at three different temperatures, of cultures at the initial time (t_0) and after 75 min of exposure at 95 cm from the solar simulator, under three radiation treatments, receiving 184 µmol photons m^{-2} s^{-1}), 35 and 0.64 W m^{-2} for PAR, UV-A and UV-B, respectively. Closed and open symbols represent LL- (100 µmol photons m^{-2} s^{-1}) and HL- (250 µmol photons m^{-2} s^{-1}) acclimated samples, respectively. The symbols show mean values with the standard deviation.

rates were observed during the E2 experiments as compared to E1, especially in samples receiving UVR. In general, higher recovery rates were determined (within the same temperature treatment) in cells pre-acclimated to LL and exposed to the lower irradiance in E2, and cells pre-acclimated to HL in E1 (except for 25 °C, Fig. 4E) as compared to all other treatments. Samples under the P treatment did not display a clear pattern, and in some cases they even had a decrease in recovery rates (e.g., at 25 °C after LL pre-acclimation, Fig. 4F).

rETR curves were obtained with cells from the different treatments during E1 (Fig. 5). The general trend was that $rETR_{max}$ was reached at relatively low irradiances and decreased afterwards relatively fast. After the exposure, the rETR vs. *I* curves showed lower $rETR_{max}$ values than at t_0 in almost all the treatments, together with an upward trend in I_k towards higher irradiances. Samples under the P treatment had higher $rETR_{max}$ than the samples receiving UVR at all temperatures and when compared within the same pre-acclimation condition (Fig. 5). Under the LL pre-acclimation condition, the $rETR_{max}$ for samples under PAR was higher at 20 °C (Fig. 5C) than under the other temperatures (Fig. 5A and E). It is interesting to note that at 25 °C (Fig. 5E) there was a measurable $rETR_{max}$ in samples exposed to UVR, while at the lower temperatures these values were zero (Fig. 5A and C). In the case of HL pre-acclimated samples, $rETR_{max}$ decreased from 15 °C (Fig. 5B) to 25 °C (Fig. 5F).

In the motility experiments, no significant changes in the swimming velocity were observed during the exposure and recovery period (Fig. 6) regardless of the treatment of the cells. However, in general, the swimming velocity was higher at 15° and 20 °C (Fig. 6A–D) ($p < 0.05$) than at 25 °C (Fig. 6E and F). Furthermore, no apparent effect of any treatment was observed in the percentage of motile cells (data not shown).

4. Discussion

Our experiments, designed to assess the combined impact of increased radiation levels and temperature in cells with two different light histories, used an experimental set up mimicking different conditions of decreasing depth in the upper mixed layer (UML). Such a decrease in the UML depth, as a result of increasing temperature in a global change scenario has been already predicted [29], taken into account that the mean annual temperature in the oceans has risen constantly since 1900 by about 1 °C [37]. These temperature increases are expected to alter aquatic ecosystems in terms of biomass productivity and species composition [38–40]. It is also expected that algal blooms will increase in frequency with global warming [41,42], because of several associated phenomena such as longer seasons of elevated temperatures and the increased vertical stratification intensity [41].

The rationale behind the experimental set up and the selected target organism was based on previous data obtained for the Patagonian coast: In mid latitudes of Patagonia the depth of the UML is variable due to the combination of wind and solar heating [43]) thus we could expect such changes in the UML as we tested in our experiments. Moreover, various combinations of attenuation coefficients together with the incident solar radiation, mainly

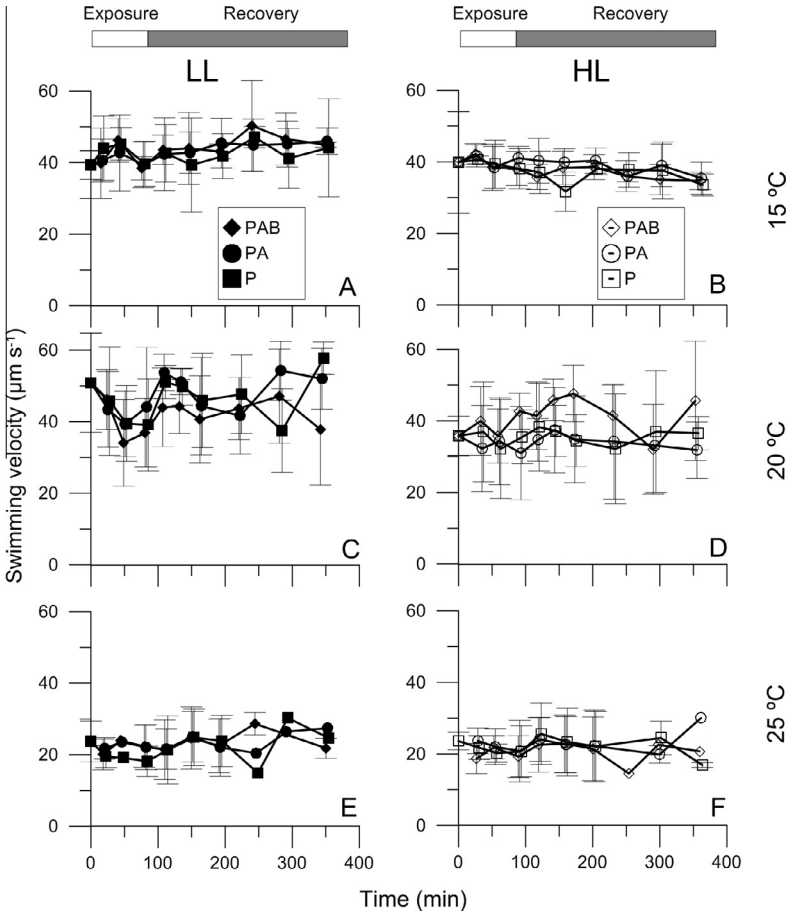

Fig. 6. Swimming velocity ($\mu m\ s^{-1}$) during exposure and recovery of samples exposed at 95 cm from the solar simulator, under three radiation treatments, receiving 184 (846 µmol photons $m^{-2}\ s^{-1}$), 35 and 0.64 W m^{-2} for PAR, UV-A and UV-B, respectively, at 15, 20 and 25 °C. Closed and open symbols represent LL- and HL-acclimated samples, respectively. Symbols indicate mean values of the different radiation treatments (P squares, PA circles, PAB diamonds) with standard deviation.

modulated by clouds, can result in variable levels of radiation such as those used in our experiments. It should be noted, however, that we used an attenuation coefficient for PAR to establish the levels of irradiance, but solar radiation is attenuated differentially, with UVR wavelengths being attenuated stronger in the water column [44]. In coastal waters this attenuation is enhanced, depending on the concentration of dissolved organic matter (DOM) and particulate material [45]. Nevertheless, the proportion of energy received in our experiments (UV-B/UV-A/PAR of 1/54/287 W m^{-2}) is comparable to the ones measured at mid latitudes (i.e., 1/34/235 W m^{-2}) [46]. So, in our experiments, cells received slightly more UVR than in their natural habitats. Regarding the organism used for this study i.e., a dinoflagellate, it is an important component of the phytoplankton community in Patagonia during summer [47]. Moreover, dinoflagellates are known to produce blooms ([48]) and/or toxic events ([49]) thus, the implications of our work are obvious to understand the physiology of key organisms in a global change scenario as we proposed in this study.

Our results show clearly that the effective photochemical quantum yield for PSII decreases significantly during radiation exposure and recovers during the subsequent dim light period. As expected, the inhibition was largest and the recovery slowest for samples receiving UVR, and to a lesser extend to the ones receiving only PAR, as seen in many studies (see review by Villafañe et al. [50]). However, both the degree of inhibition and recovery strongly depended on the light history (low or high irradiance during the acclimation period) and the temperature. Samples pre-acclimated to HL showed in general less inhibition and higher recovery than those pre-acclimated to LL. Various studies either speculated with this and/or conducted experiments to determine the role of the previous light history [51]. The acclimation processes involve many factors, which include the synthesis of UV-absorbing compounds under high irradiance conditions [52] as well as a higher epoxidation and epoxidation rates involving the xanthophyll cycle [53]. These mechanisms help high light acclimated cells to cope with the excess radiation stress which thus have a better photosynthetic performance.

However, and as mentioned before, temperature also plays an important role in the observed results, and regardless of the light acclimation levels, *G. clorophorum* had a better performance at 20 °C in our controls (i.e., PAR exposed cells), with higher yield and $rETR_{max}$, than samples incubated at 15 or 25 °C. However, the combined effects of increased UVR and temperature were different depending on the light history. For example, cells pre-acclimated to LL had a complete inhibition in samples exposed to UVR (i.e., PAB and PA treatments) at 15 and 20 °C (Fig. 5). However, the increased temperature acted antagonistically with UVR, and low values of rETR could be measured (Fig. 5). In contrast, in HL pre-acclimated cells, the inhibition was lower and rETR values were measured at all temperatures (Fig. 5). This differential interactive effect between temperature and UVR, points to a situation in which opaque environments, with relative low mean irradiances within the UML, the cells might benefit from an increase in temperature to counteract the negative effects of UVR.

Short wavelengths of solar radiation, especially UV-B, affect many physiological and morphological functions in phytoplankton [54–56]. Cellular targets are proteins and lipids [57], the nuclear, mitochondrial and chloroplast DNA [58,59] and the photosynthetic apparatus [47,60]. Solar UV-B has been found to damage the D1 protein, involved in the electron transport chain in photosystem II [61], which is subsequently proteolytically removed from its site, reducing the overall photosynthetic electron transport rate and the quantum yield and biomass productivity [62]. Previous studies [63,64] have shown that increased temperature can counteract some of these negative UVR effects, as an increased metabolic activity help the cell to cope with UVR. However, this is not always the case, as increased temperatures might in fact act synergistically with UVR, further harming cells growing at their upper limit of temperature tolerance [65].

Many phytoplankton organisms use active or passive migration to optimize their vertical position in the water column with respect to the light intensity using either active swimming [66] or changes in buoyancy [67,68]. Dinoflagellates, such as *Peridinium*, *Amphidinium* and *Prorocentrum* use phototaxis and gravitaxis to move upward or downward in the water column depending on the prevalent irradiance [69,70]. However, exposure to excessive solar PAR and UVR impairs both the orientation mechanisms and the motility in flagellates [71,72]. However, at the irradiance levels used during the exposure of *Gymnodinium* in the present study, no inhibition of swimming velocity or the percentage of motile cells was detected.

5. Conclusions

Our results indicate that the previous light history of exposure of the cells is critical at the time to determine their response to the combined impact of increasing UVR and temperature, with their interactive effects changing from antagonistic (in LL-acclimated cells) to synergistic (in HL-acclimated cells). Particularly, when evaluating photochemical responses, the degree of inhibition and recovery strongly depends on the previous light history of the cells and the prevalent water temperature, supporting the notion that phytoplankton abundance and productivity is significantly affected by global climate change [73,74]. Since different taxa and cellular targets have different sensitivities to variations in environmental factors, changes in the species composition as well as in physiological responses, due to climate change, are to be expected, with significant consequences for the whole food web in the aquatic ecosystems [75,76].

Acknowledgements

We thank for the comments and suggestions by three anonymous reviewers as well as those from Dr. D. Campbell that helped to improve our manuscript. This work was supported by Consejo Nacional de Investigaciones Científicas y Técnicas (CONICET) – Deutsche Forschungsgemeinschaft (DFG), Agencia Nacional de Promoción Científica y Tecnológica – ANPCyT (PICT 2007-1651, and PICT 2012-0271), CONICET PIP 11220100100228, and Fundación Playa Unión. This is Contribution N° 138 of Estación de Fotobiología Playa Unión.

References

[1] D.-P. Häder, E.W. Helbling, C.E. Williamson, R.C. Worrest, Effects of UV radiation on aquatic ecosystems and interactions with climate change, Photochem. Photobiol. Sci. 10 (2011) 242–260.
[2] M. Behrenfeld, R. O'Malley, D. Siegel, C. McClain, J. Sarmiento, G. Feldman, A. Milligan, P. Falkowski, R. Letelier, E. Boss, Climate-driven trends in contemporary ocean productivity, Nature 444 (2006) 752–755.
[3] P.G. Falkowski, J.A. Raven, Aquatic photosynthesis, Blackwell Science, Massachusetts, US, 1997.
[4] F. Azam, Microbial control of oceanic carbon flux: the plot thickens, Science 280 (1998) 694–696.
[5] M.J.H. van Oppen, F.P. Palstra, A.M.T. Piquet, D.J. Miller, Patterns of coral-dinoflagellate associations in *Acropora*: significance of local availability and physiology of *Symbiodinium* strains and host-symbiont selectivity, Proc. Royal Soc. London B 268 (2001) 1759–1767.
[6] D.-I. Kim, Y. Matsuyama, S. Nagasoe, M. Yamaguchi, Y.-H. Yoon, Y. Oshima, N. Imada, T. Honjo, Effects of temperature, salinity and irradiance on the growth of the harmful red tide dinoflagellate *Cochlodinium polykrikoides* Margalef (Dinophyceae), J. Plankton Res. 26 (2004) 61–66.
[7] K.A. Steidinger, J.H. Landsberg, E.W. Truby, B.S. Roberts, First report of *Gymnodinium pulchellum* (Dinophyceae) in North America and associated fish kills in the Indian River, Florida, J. Phycol. 34 (1998) 431–437.

[8] G.M. Hallegraeff, Ocean climate change, phytoplankton community responses, and harmful algal blooms: a formidable predictive challenge, J. Phycol. 46 (2010) 220–235.

[9] S.C.Y. Leong, A. Murata, Y. Nagashima, S. Taguchi, Variability in toxicity of the dinoflagellate *Alexandrium tamarense* in response to different nitrogen sources and concentrations, Toxicon 43 (2004) 407–415.

[10] J.M. Drake, D.M. Lodge, Global hot spots of biological invasions: evaluating options for ballast-water management, Proc. Royal Soc. London B 271 (2004) 575–580.

[11] D.C.R. Hauser, M. Levandowsky, S.H. Hutner, L. Chunosoff, J.S. Hollwitz, Chemosensory responses by the heterotrophic marine dinoflagellate *Crypthecodinium cohnii*, Microbial Ecol. 1 (1975) 246–254.

[12] H.J. Jeong, The ecological roles of heterotrophic dinoflagellates in marine planktonic community, J. Eukaryotic Microbiol. 46 (1999) 390–396.

[13] R. Cortés-Altamirano, R. Alonso-Rodríguez, Mareas rojas durante, En la Bahía de Mazatlán, Sinaloa, México, Ciencia Marina 15 (1997) (1997) 31–37.

[14] J.H. Landsberg, K. Steidinger, A historical review of *Gymnodinium breve* red tides implicated in mass mortalities of the manatee (*Trichechus manatus latirostris*) in Florida, Harmful Algae, USA, 1998. 97–100.

[15] J. Iriarte, H. González, Phytoplankton bloom ecology of the Inner Sea of Chiloe, Southern Chile, Nova Hed. Beihefte 133 (2008) 67.

[16] C.J. Band-Schmidt, J.J. Bustillos-Guzmán, D.J. López-Cortés, I. Gárate-Lizárraga, E.J. Núñez-Vázquez, F.E. Hernández-Sandoval, Ecological and physiological studies of *Gymnodinium catenatum* in the Mexican Pacific: a review, Mar. Drugs 8 (2010) 1935–1961.

[17] L. MacKenzie, L. Rhodes, The Intergovernmental Oceanographic Commission of UNESCO: Harmful Algae News. An IOC Newsletter on toxic algae and algal blooms, No. 7, 1993, p. 2.

[18] S. Nehring, (Ed.), The Intergovernmental Oceanographic Commission of UNESCO: Harmful Algae News. An IOC Newsletter on Toxic Algae and algal Blooms, No. 7, 1993, pp. 1–4.

[19] J. Schäfer, C. Sebastian, D.-P. Häder, Effects of solar radiation on motility, orientation, pigmentation and photosynthesis in a green dinoflagellate *Gymnodinium*, Acta Protozool. 33 (1993) 59–65.

[20] E.W. Helbling, A.G.J. Buma, W. Van de Poll, M.V. Fernández Zenoff, V.E. Villafañe, UVR-induced photosynthetic inhibition dominates over DNA damage in marine dinoflagellates exposed to fluctuating solar radiation regimes, J. Exp. Mar. Biol. Ecol. 365 (2008) 96–102.

[21] J.N. Bouchard, C. García-Gómez, M.R. Lorenzo, M. Segovia, Differential effect of ultraviolet exposure (UVR) in the stress response of the Dinophycea *Gymnodinium* sp. and the Chlorophyta *Dunaliella tertiolecta*: mortality versus survival, Mar. Biol. 160 (2013) 2547–2560.

[22] T.J. Evens, G.J. Kirkpatrick, D.F. Millie, D.J. Chapman, O.M. Schofield, Photophysiological responses of the toxic red-tide dinoflagellate *Gymnodinium breve* (Dinophyceae) under natural sunlight, J. Plankton Res. 23 (2001) 1177–1194.

[23] P.R. Richter, D.-P. Häder, R.J. Goncalves, M.A. Marcoval, V.E. Villafañe, E.W. Helbling, Vertical migration and motility responses in three marine phytoplankton species exposed to solar radiation, Photochem. Photobiol. 83 (2007) 810–817.

[24] R.P. Dunne, Synergy or antagonism-interactions between stressors on coral reefs, Coral Reefs 29 (2010) 145–152.

[25] S.L. Hinder, G.C. Hays, M. Edwards, E.C. Roberts, A.W. Walne, M.B. Gravenor, Changes in marine dinoflagellate and diatom abundance under climate change, Nat. Clim. Change 2 (2012) 271–275.

[26] E. Litchman, P.J. Neale, A.T. Banaszak, Increased sensitivity to ultraviolet radiation in nitrogen-limited dinoflagellates: photoprotection and repair, Limnol. Oceanogr. 47 (2002) 86–94.

[27] S.A. Doyle, J.E. Saros, C.E. Williamson, Interactive effects of temperature and nutrient limitation on the response of alpine phytoplankton growth to ultraviolet radiation, Limnol. Oceanogr. 50 (2005) 1362–1367.

[28] M. Elbrächter, E. Schnepf, *Gymnodinium chlorophorum*, a new, green, bloom-forming dinoflagellate (Gymnodiniales, Dinophyceae) with a vestigial prasinophyte endosymbiont, Phycologia 35 (1996) 381–393.

[29] J. Beardall, C. Sobrino, S. Stojkovic, Interactions between the impacts of ultraviolet radiation, elevated CO_2, and nutrient limitation on marine primary producers, Photochem. Photobiol. Sci. 8 (2009) 1257–1265.

[30] R.R.L. Guillard, J.H. Ryther, Studies of marine planktonic diatoms. I. *Cyclotella nana* Hustedt and *Detonula convervacea* (Cleve) Gran, Can. J. Microbiol. 8 (1962) 229–239.

[31] P.J. Neale, E.W. Helbling, H.E. Zagarese, in: E.W. Helbling, H.E. Zagarese (Eds.), UV effects in aquatic organisms and ecosystems, Royal Society of Chemistry, 2003, pp. 108–134.

[32] E.W. Helbling, D.E. Pérez, C.D. Medina, M.G. Lagunas, V.E. Villafañe, Phytoplankton distribution and photosynthesis dynamics in the Chubut River estuary (Patagonia, Argentina) throughout tidal cycles, Limnol. Oceanogr. 55 (2010) 55–65.

[33] B. Genty, J.M. Briantais, N.R. Baker, The relationship between the quantum yield of photosynthetic electron transport and quenching of chlorophyll fluorescence, Biochim. Biophys. Acta 990 (1989) 87–92.

[34] E. Weis, A. Berry, Quantum efficiency of photosystem II in relation to the energy dependent quenching of chlorophyll fluorescence, Biochim. Biophys. Acta 894 (1987) 198–208.

[35] P. Eilers, J. Peeters, A model for the relationship between light intensity and the rate of photosynthesis in phytoplankton, Ecol. Mod. 42 (1988) 199–215.

[36] M. Lebert, D.-P. Häder, Image analysis: a versatile tool for numerous applications, G.I.T. Imag. Micros. 1 (1999) 5–6.

[37] M. Fischetti, Deep heat threatens marine life, Sci. Am. 2013 (2013) 72.

[38] R. Müller, T. Laepple, I. Bartsch, C. Wiencke, Impact of global climate change on the distribution of seaweeds in polar and cold-temperate waters, Bot. Mar. 52 (2009) 617–638.

[39] J. Beardall, S. Stojkovic, S. Larsen, Living in a high CO_2 world: impacts of global climate change on marine phytoplankton, Plant Ecol. Divers. 2 (2009) 191–205.

[40] R.J. Goncalves, M.S. Souza, J. Aigo, B. Modenutti, E. Balseiro, V.E. Villafañe, V. Cussac, E.W. Helbling, Responses of plankton and fish and temperate zones to UVR and temperature in a context of global change, Ecol. Aust. 20 (2010) 129–153.

[41] H. Paerl, J. Scott, Throwing fuel on the fire: synergistic effects of excessive nitrogen inputs and global warming on harmful algal blooms, Environ. Sci. Technol. 44 (2010) 7756–7758.

[42] M. Kahru, V. Brotas, B. Manzano-Sarabia, B.G. Mitchell, Are phytoplankton blooms occurring earlier in the Arctic?, Global Change Biol 17 (2010) 1733–1739.

[43] V.E. Villafañe, E.S. Barbieri, E.W. Helbling, Annual patterns of ultraviolet radiation effects on temperate marine phytoplankton off Patagonia, Argentina, J. Plankton Res. 26 (2004) 167–174.

[44] J.T.O. Kirk, The vertical attenuation of irradiance as a function of the optical properties of the water, Limnol. Oceanogr. 48 (2003) 9–17.

[45] C.L. Osburn, D.P. Morris, in: E.W. Helbling, H. Zagarese (Eds.), UV effects in aquatic organisms and ecosystems, The Royal Society of Chemistry, Cambridge, 2003, pp. 185–217.

[46] D.-P. Häder, M. Lebert, M. Schuster, L. del Ciampo, E.W. Helbling, R. McKenzie, ELDONET – a decade of monitoring solar radiation on five continents, Photochem. Photobiol. 83 (2007). 1384–1357.

[47] V.E. Villafañe, P.J. Janknegt, M. de Graaff, R.J.W. Visser, W.H. van de Poll, A.G.J. Buma, E.W. Helbling, UVR-induced photoinhibition of summer marine phytoplankton communities from Patagonia, Mar. Biol. 154 (2008) 1021–1029.

[48] J.L. Iriarte, R.A. Quiñones, R.R. González, Relationship between biomass and enzymatic activity of a bloom-forming dinoflagellate (Dinophyceae) in southern Chile (41 S): a field approach, J. Plankton Res. 27 (2005) 1–8.

[49] J.L. Esteves, N. Santinelli, V. Sastre, R. Díaz, O. Rivas, A toxic dinoflagellate bloom and PSP production associated with upwelling in Golfo Nuevo, Patagonia, Argentina, Hydrobiologia 242 (1992) 115–122.

[50] V.E. Villafañe, K. Sundbäck, F.L. Figueroa, E.W. Helbling, in: E.W. Helbling, H.E. Zagarese (Eds.), UV effects in aquatic organisms and ecosystems, Royal Society of Chemistry, 2003, pp. 357–397.

[51] A.G.J. Buma, R.J. Visser, W. Van de Poll, V.E. Villafañe, P.J. Janknegt, E.W. Helbling, Wavelength-dependent xanthophyll cycle activity in marine microalgae exposed to natural ultraviolet radiation, Eur. J. Phycol. 44 (2009) 515–524.

[52] E.W. Helbling, B.E. Chalker, W.C. Dunlap, O. Holm-Hansen, V.E. Villafañe, Photoacclimation of antarctic marine diatoms to solar ultraviolet radiation, J. Exp. Mar. Biol. Ecol. 204 (1996) 85–101.

[53] W.H. Van de Poll, A.G.J. Buma, Does ultraviolet radiation affect the xanthophyll cycle in marine phytoplankton?, Photochem Photobiol. Sci. 8 (2009) 1295–1301.

[54] H. Harada, M. Vila-Costa, J. Cebrian, R.P. Kiene, Effects of UV radiation and nitrate limitation on the production of biogenic sulfur compounds by marine phytoplankton, Aquat. Bot. 90 (2009) 37–42.

[55] C.E. Williamson, C. Salm, S.L. Cooke, J.E. Saros, How do UV radiation, temperature, and zooplankton influence the dynamics of alpine phytoplankton communities?, Hydrobiologia 648 (2010) 73–81

[56] P. Echeveste, S. Agustí, J. Dachs, Cell size dependence of additive versus synergetic effects of UV radiation and PAHs on oceanic phytoplankton, Envirom. Pollut. 159 (2011) 1307–1316.

[57] J.N. Bouchard, S. Roy, G. Ferreyra, D.A. Campbell, A. Curtosi, Ultraviolet-B effects on photosystem II efficiency of natural phytoplankton communities from Antarctica, Polar Biol. 28 (2005) 607–618.

[58] M. Vernet, S. Díaz, H. Fuenzalida, C. Camilión, C.R. Booth, S. Cabrera, C. Casicca, G. Defarrari, C. Lovengreen, A. Paladini, J. Pedroni, A. Rosales, H. Zagarese, Quality of UVR exposure for different biological systems along a latitudinal gradient, Photochem. Photobiol. Sci. 8 (2009) 1329–1345.

[59] J.A. Meador, A.J. Baldwin, P. Catala, W.H. Jeffrey, F. Joux, J.A. Moss, J.D. Pakulski, R. Stevens, D.L. Mitchell, Sunlight-induced DNA damage in marine micro-organisms collected along a latitudinal gradient from 70 degrees N to 68 degrees S, Photochem. Photobiol. 85 (2009) 412–421.

[60] W. Zhou, K. Yin, X. Yuan, X. Ning, Comparison of the effects of short-term UVB radiation exposure on phytoplankton photosynthesis in the temperate Changjiang and subtropical Zhujiang estuaries of China, J. Oceanogr. 65 (2009) 627–638.

[61] J.N. Bouchard, S. Roy, D.A. Campbell, UVB effects on the photosystem II-D1 protein of phytoplankton and natural phytoplankton communities, Photochem. Photobiol. 82 (2006) 936–951.

[62] S. Wängberg, J.S. Selmer, K. Gustavson, Effects of UV-B radiation on biomass and composition in marine phytoplankton communities, Sci. Mar. 60 (suppl. 1) (1996) 81–88.

[63] S.R. Halac, V.E. Villafañe, E.W. Helbling, Temperature benefits the photosynthetic performance of the diatoms *Chaetoceros gracilis* and

Thalassiosira weissflogii when exposed to UVR, J. Photochem. Photobiol. B: Biol. 101 (2010) 196–205.
[64] E.W. Helbling, A.G.J. Buma, P. Boelen, H.J. van der Strate, M.V. Fiorda Giordanino, V.E. Villafañe, Increase in Rubisco activity and gene expression due to elevated temperature partially counteracts ultraviolet radiation–induced photoinhibition in the marine diatom *Thalassiosira weissflogii*, Limnol. Oceanogr. 56 (2011) 1330–1342.
[65] S.R. Halac, S.D. Guendulain-García, V.E. Villafañe, E.W. Helbling, A.T. Banaszak, Responses of tropical plankton communities from the Mexican Caribbean to solar ultraviolet radiation exposure and increased temperature, J. Exp. Mar. Biol. Ecol. 445 (2013) 99–107.
[66] D.-P. Häder, K. Griebenow, Orientation of the green flagellate, *Euglena gracilis*, in a vertical column of water, FEMS Microbiol. Ecol. 53 (1988) 159–167.
[67] R. Kinsman, B.W. Ibelings, A.E. Walsby, Gas vesicle collapse by turgor pressure and its role in buoyancy regulation by *Anabaena flos-aquae*, J. Gen. Microbiol. 137 (1991) 1171–1178.
[68] A.E. Walsby, in: P. Fay, C. Van Baalen (Eds.), The Cyanobacteria, Elsevier Science, Publishers, 1987, pp. 385–392.
[69] B. Eggersdorfer, D.-P. Häder, Phototaxis, gravitaxis and vertical migrations in the marine dinoflagellates, *Peridinium faeroense* and *Amphidinium caterea*, Acta Protozool. 30 (1991) 63–71.
[70] B. Eggersdorfer, D.-P. Häder, Phototaxis, gravitaxis and vertical migrations in the marine dinoflagellate *Prorocentrum micans*, FEMS Microbiol. Ecol. 85 (1991) 319–326.
[71] R.A. Danilov, N.G.A. Ekelund, Effects of increasing doses of UV-B radiation on photosynthesis and motility in *Clamydomonas reinhardtii*, Folia Microbiol. 45 (2000) 41–44.
[72] P. Richter, W. Helbling, C. Streb, D.-P. Häder, PAR and UV effects on vertical migration and photosynthesis in *Euglena gracilis*, Photochem. Photobiol. 83 (2007) 818–823.
[73] M.J. Behrenfeld, T.K. Westberry, E.S. Boss, R.T. O'Malley, D.A. Siegel, J.D. Wiggert, B.A. Franz, C.R. McClain, G.C. Feldman, S.C. Doney, J.K. Moore, G. Dall'Olmo, A.J. Milligan, I. Lima, N. Mahowald, Satellite-detected fluorescence reveals global physiology of ocean phytoplankton, Biogeosciences 6 (2009) 779–794.
[74] M. Montes-Hugo, S.C. Doney, H.W. Ducklow, W. Fraser, D. Martinson, S.E. Stammerjohn, O. Schofield, Recent changes in phytoplankton communities associated with rapid regional climate change along the Western Antarctic Peninsula, Science 323 (2009) 1470–1473.
[75] C. Belzile, S. Demers, G.A. Ferreyra, I. Schloss, C. Nozais, K. Lacoste, B. Mostajir, S. Roy, M. Gosselin, E. Pelletier, S.M.F. Gianesella, M. Vernet, UV effects on marine planktonic food webs: a synthesis of results from mesocosm studies, Photochem. Photobiol. 82 (2006) 850–856.
[76] M.-Y. Sun, L.M. Clough, M.L. Carroll, J. Dai, W.G. Ambrose Jr., G.R. Lopez, Different responses of two common Arctic macrobenthic species (*Macoma balthica* and *Monoporeia affinis*) to phytoplankton and ice algae: will climate change impacts be species specific? J. Exp. Mar. Biol. Ecol. 376 (2009) 110–121.